

PROCEEDINGS
of the
TECHNICAL PROGRAM

**ELECTRO-OPTICAL SYSTEMS DESIGN
CONFERENCE - 1971 WEST**

ANAHEIM, CALIFORNIA

•

MAY 18, 19, 20, 1971

PROCEEDINGS
of the
TECHNICAL PROGRAM

**ELECTRO-OPTICAL SYSTEMS DESIGN
CONFERENCE - 1971 WEST**

ANAHEIM, CALIFORNIA • MAY 18, 19, 20, 1971

This first Electro-Optics West Conference was an outstanding success. The attendance was excellent, the exhibition featured sophisticated and practical products from all areas of the technology, and the technical sessions were well attended by the West Coast designers. The papers given at the technical sessions are contained in this technical proceedings. There are 59 papers grouped in twelve technical sessions. Some sessions are quite large because of the large number of excellent papers that were received in these areas.

The largest session was concerned with lasers. Here, eleven papers surveyed the technology that goes into producing both good and practical lasers. Two papers discussed the struggling field of laser diodes; others were concerned with traveling wave UV lasers, parametric tuning of lasers and the applications of photomultipliers in the measurement of laser parameters.

As has been true in other EO conferences, the low light level TV session attracted the highest attendance. The highlight of this session was a round table discussion, comprised of individuals from industry and the military, that put the whole area of LLLTV into a very practical light. The panel discussed not only the problem areas and possible solutions, but also where the LLLTV would be making excellent contributions in the near future.

Another especially well-attended session dealt with atmospheric optics. Ten papers were given and the interest was high in all of them.

As usual, the infrared detector session was well attended. Here, the emphasis was on lead tin telluride detectors, miniaturized detectors and current, as well as future applications.

Many other sessions had special features, but unfortunately, we do not have sufficient space to mention them individually.

Credit for the excellent set of papers and the resulting attendance at the conference must be given to E-O consultant Art Kaufman, who coordinated the entire effort, and to each session chairman, who spent many hours of time and effort to insure not only that the papers were technically excellent, but also were well written and presented.

The Conference staff and the session chairmen wish to thank the authors for their time and effort. A special thanks goes to the electro-optical companies who allowed the authors time to develop their papers and defrayed their expenses.

This Proceedings is an industry-wide effort and without the cooperation of many firms, this undertaking would be impossible and this excellent set of papers would not be available for reference in the years ahead.

Milton S. Kiver
Conference Chairman

TABLE OF CONTENTS

SESSION I: LASER TECHNOLOGY*

Chairman: Dr. Arnold L. Bloom, Spectra Physics, Inc.

A Traveling Wave Vacuum Ultraviolet Laser, by Ronald W. Waynant	1
Room Temperature GaAlAs Close-Confinement Laser Diodes, by R. Gill, T. Gonda, P. Nyul, A. Limm and R. Speers	6
Moderate-Power GaAlAs Laser Diode Array Light Sources, by A. Limm, P. Nyul, R. Gill and T. Gonda	13
Flash Lamp Circuit Design, by J. P. Markiewicz	20
Tuning of Optical Parametric Fluorescence in Uniaxial Crystals, by Carl F. Dadson and R. J. Anderson	30
High Efficiency Laser Polarizer, by Jerome Swartz, Donald K. Wilson and Richard J. Kapash	35
Photographic Response of Certain Films to Q-Switched Ruby Laser Energy, by Clarence E. Robertson	39
Photomultipliers with GaInAs Photocathodes for Use in the Near Infrared, by D. E. Persyk and F. R. Hughes	48
Negative Electron Affinity Photocathodes in Photomultiplier Tubes, by T. T. Lewis	56
Change in Photomultiplier Area Sensitivity Map with Wavelength of Illumination, by Otto Youngbluth, Jr.	60

SESSION II: ATMOSPHERIC OPTICS & AEROSOL SCATTERING--SESSION I

Chairman: Dr. E. Ronald Atkinson, Naval Weapons Center

Propagation of Focused Laser Beams, by H. Shenker, J. A. Dowling and J. A. Curcio	67
The Beam Wander Phenomenon in the Turbulent Near-Earth Atmosphere, by Ernest C. Alcaraz and Peter M. Livingston	76
A High Altitude Raindrop Analyzer Experiment, by W. L. Teeter and H. B. Glenn	81
Models for Absorption Hygrometry, by Arden L. Buck	88

SESSION III: COHERENT OPTICS

Chairman: Dr. Brian J. Thompson, University of Rochester

An Introduction to Coherent Optical Systems, by Brian J. Thompson	97
Flaw Detection Sensitivity of Holographic Interferometry on Cylinders Under Hoop Stress, by C. G. Murphy, O. J. Burchett and C. W. Matthews	101

*Prepared by the Laser Industry Association

Strain Measurement by Optical Correlation Methods, by R. K. Mueller and T. Sawatari	108
Holography as a Tool in the Verification of a Model of Red Cell Rotation, by Dr. M. O. Breitmeyer and M. K. Sambandam	115
Salicylideneaniline as a Data Storage Medium, by D. S. Lo, D. M. Manikowski and M. M. Hanson	122
<u>SESSION IV:</u>	<u>RECENT ADVANCES IN INFRARED DETECTORS AND INFRARED SYSTEMS</u>
Chairman: Eric M. Wormser, Barnes Engineering Co.	
Infrared Detectors of PbSnTe Sensitive in the 8-14 Micron Spectral Region, by K. J. Linden and P. P. Debye	127
A Status Report on InSb and PbSnTe Detector Developments, by J. E. Slawek and Paul Chia	139
High Performance Miniature Infrared Sensors, by R. A. Bell and D. B. Williams	145
Infrared Systems for the Future, by R. D. Hudson, Jr.	154
The Infrared Radiometer Experiment for the Mariner 1971 Mars Orbiter Mission, by Stillman C. Chase, Jr.	157
ITOS Meteorological Scanning Radiometer, by LeRoy Barncastle	164
Precision LWIR Calibration and Test, by William R. Williamson and Allen A. Otte	174
<u>SESSION V:</u>	<u>SYSTEMS APPLICATIONS OF LASERS*</u>
Chairman: Dr. Althur Lubin, Hadron Inc.	
Intercept Receiver Requirements for E-O Countermeasures, by Hanns J. Wetzstein	181
Modulated Laser Beam Wideband Recording System, by H. W. Pass and L. R. Teeple, Jr.	195
Effectiveness of IR Covert Illuminators, by F. J. Gardiner	202
Laser Optical Systems to Measure Surface Erosion of Hypervelocity Models in the 1000-Foot Hyperballistics Range, by Robert R. Gastrock	208
<u>SESSION VI:</u>	<u>ATMOSPHERIC OPTICS AND AEROSOL SCATTERING--SESSION 2</u>
Chairman: Dr. E. Ronald Atkinson, Naval Weapons Center	
Temporal Profiles of Aerosol Backscatter, by H. H. Burroughs	215
Particle Size Measurements From Aircraft Using Electro-Optical Techniques, by R. G. Knollenberg	218
A Liquid-Crystal Light Valve, by D. W. Peterson	234

*Prepared by the Laser Industry Association

SESSION VII: LLL IMAGING

Chairman: Herbert P. Lavin, General Electric Co.

Comparison of Low Light Level Television Systems, by Harold V. Soule	239
A New S-25 Television Tube, by John F. Spalding	246
Modulation Transfer Function of Low Light Level Imaging Systems, by N. S. Kapany, B. G. Phillips and B. J. Tullis	249
Application of Television Techniques to Auroral Research, by Thomas J. Hallinan and Larry R. Sweet	268

SESSION VIII: COMPUTER OUTPUT MICROFILM

Chairman: Joseph E. Eichberger, Extek Microsystems, Inc.

Recording Media for Use in COM Systems, by Sherman H. Boyd	275
Low Cost COM Recorders, by Paul Seitz	285
A New Device for Microfilm Storage and Retrieval, by Robert A. Morgan	292

SESSION IX: INDUSTRIAL APPLICATIONS OF LASERS*

Chairman: Russell Targ, Sylvania Electronic Products, Inc.

Industrial Applications of High Power Lasers	301
Surface Topography Diagnostics in the Manufacture of Film Integrated Circuits Using Scanned Focussed Lasers, by D. F. Munro and J. D. Cuthbert	311
Measurement of the Parallelism of the Two Surfaces of Optical Components Using Nonlocalized Fringes Produced by a Laser, by C. S. Willett, J. H. Wasilik and T. V. Blomquist	318
An Electro-Optical Distance Measuring Instrument for Surveying, by Robin H. Hines and William L. Hollinshead	324

SESSION X: UNDERWATER ELECTRO-OPTICS **

Chairmen: Charles N. DeMund, General Dynamics/Convair
 Dr. Seibert Q. Duntley, Scripps Institute of Oceanography

Deep Submergence Windows for Optical Systems, by Joe J. Lones and J. D. Stachiw	329
Exposure Controls for Underwater Photography, by Robert L. Adams and William G. Hulburd	336
Optical Turbulence in the Sea, by Gary D. Gilbert and Richard C. Honey	340

*Prepared by the Laser Industry Association

**Prepared by the Society of Photo-Optical Instrumentation Engineers

SESSION XI: ADVANCES IN SOLID STATE DETECTORS AND APPLICATIONS

Chairman: John O'Brien, EG&G

The Schottky Barrier Silicon Photodetector in Perspective with Other Detection Devices in the 200 to 1100 Range, by Philip H. Davis	349
Temperature Effects Upon Partially and Fully Depleted Silicon Photodetectors, by Ralph M. Mindock and Joseph B. Horak	357
Beam-Lead Light Sensor Arrays, by Millis Miller	373
Integrated Photodiode-Preamplifier Combinations, by A. A. Aponick, Jr. and H. L. Hardway	378
Design Aspects of the Mars Viking Lander Camera System, by Robert C. Beal	384
A Silicon Avalanche Detector-Tunnel Diode Rangefinder Receiver, by E. J. Savitsky and R. G. Trapani	393

SESSION XII: ADVANCES IN INFORMATION DISPLAY

Chairman: Leo Beiser, CBS Laboratories

Visual Binocular Disparity Tolerances for Head-Up Displays, by Theodore Gold	399
The Aerial Optical Viewfinder, by Miles J. Mraz	407
Real-Time Direct-Viewed CRT Displays Having Holographic Properties, by H. B. Tilton	415
Television Multiplexing System, by Lorenz G. Simpkins and Bobby G. Bruckner	423
Three-Dimensional Display Techniques, by Kazuo Sayanagi	428
Fiber Optic Glow Areas, by Jack B. Wielar, II	434

A TRAVELING WAVE VACUUM ULTRAVIOLET LASER

by

Ronald W. Waynant
 Naval Research Laboratory, Plasma Physics Division
 Washington, D. C.

Introduction

For the first 10 years of their existence, laser wavelengths were confined to the far infrared, infrared, visible and near ultraviolet regions of the spectrum. Indeed, there was no method of producing stimulated emission effects below 2000 Å. In the summer of 1970, however, research groups at IBM and the Naval Research Laboratory^{1,2} almost simultaneously announced laser emission from the Lyman band (1523 - 1616 Å) of molecular hydrogen. Subsequent work at NRL has resulted in nanosecond pulses with peak powers as high as the megawatt region. In addition, the NRL system is operated in a rather unique traveling-wave manner that appears suitable for both the production of still greater powers and still shorter wavelengths.

Perhaps the greatest single reason that such short wavelength lasers were not developed previously is that the upper-state spontaneous lifetime is inversely proportional to the cube of the frequency of the transition involved. Therefore, for short wavelength (high frequency) laser transitions, spontaneous emission losses can rob the upper laser level so quickly that the inversion necessary for stimulated emission cannot occur. In addition, many times, the lower laser level has a long lifetime that makes any inversion short lived or "self-terminating." These difficulties, coupled with the inherent difficulties of working with vacuum monochromators and vacuum transmission paths, caused most laser researchers to avoid this spectral region.

While difficulties in building a vacuum ultraviolet laser are abundant, it is clear that the way to succeed is by using a fast excitation source to produce an inversion in spite of the large spontaneous losses. The "self termination" imposed by the long lower level lifetime limits the operation of the device to a pulsed mode only.

Theory of the Molecular Hydrogen Laser

The original suggestion of a vacuum ultraviolet laser came from Bazhulin, et al³, who pointed out that the energy levels of molecular hydrogen shown in Fig. 1 would be suitable for lasing in the $C^1\Pi_u - X^1\Sigma_g^+$ Werner band. Ali and Kolb⁴ carried out a detailed numerical analysis of the excitation processes involved and confirmed the hypothesis theoretically. Ali⁵ later carried out similar calculations for the $B^1\Sigma_u^+ - X^1\Sigma_g^+$ Lyman band and predicted lasing in this band also.

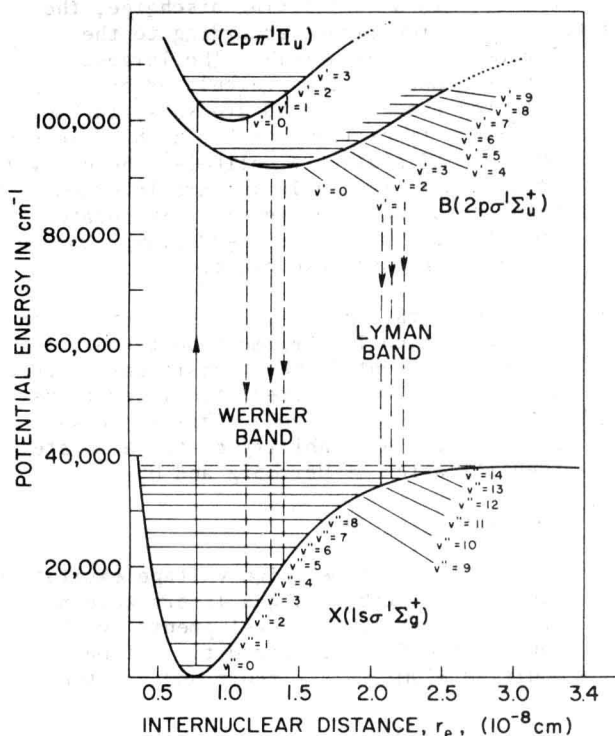


Fig. 1 (left). Energy level diagram of the hydrogen molecule showing the levels involved in vacuum ultraviolet lasing.

Table 1. Franck-Condon factors for H_2 band systems* ($B^1\Sigma_u^+ - X^1\Sigma_g^+$).

v' \ v''	0	9	10	11	12	13	14	$q_{0v'}$ $q_{v'v''}$
2	0.0273	0.2552	0.1251					0.0069, 0.0037
3	0.0427		0.2952	0.1693				0.0126, 0.0072
4	0.0563			0.3442	0.1600			0.0194, 0.0090
5	0.0663				0.4347			0.0288
6	0.0723					0.4366		0.0315
7	0.0740					0.2600		0.0192
8	0.0725						0.2781	0.020
9	0.0688							
10	0.0634							
11	0.0575						0.1546	0.0088
12	0.0513							
13	0.0452							
14	0.0394							

*The values of Franck-Condon factors were calculated by R.J. Spindler, Jr., *J. Quant. Spectrosc. Radiat. Transfer*, Vol 9, p. 620.

Without going deeply into the details of the theory, the basic process can be followed from Fig. 1. At room temperature, all the molecules are in $v'' = 0$ of $X^1\Sigma_g^+$. In a fast rising discharge, the vibrational levels in the $B^1\Sigma_u^+$ or $C^1\Pi_u$ states are populated by electron impact according to the

Franck-Condon principle. The largest Franck-Condon factors calculated by Spindler⁶ for the Lyman band are shown in Table 1. Since transitions to the high v'' levels of the $X^1\Sigma_g^+$ state are unlikely, these levels remain empty initially and are inverted with respect to the upper levels. Stimulated emission following the $v'-v''$ Franck-Condon factors can then take place.

Table 2. Laser transitions with greatest probability.

$v' \rightarrow v''$	P(1) $J'(0) - J''(1)$	P(3) $J'(2) - J''(3)$	R(1) $J'(2) - J''(1)$
2-9	1571.99	1577.4	1569.39
2-10	1623.52	1628.35	1620.75
3-10	1591.31	1596.06	1588.76
3-11	1536.33	1640.29	1633.63
4-11	1604.48	1608.39	1601.99
4-12	1641.52	1644.39	1638.90
5-12	1610.33	1613.18	1607.90
6-13	1607.50	1609.02	1605.18
7-13	1579.19	1580.74	1577.03
8-14	1567.41	1567.25	1565.35
11-14	1495.52	1495.57	1493.84

The rotational levels associated with each vibrational level must be taken into account to identify the transitions. Table 2 shows some of the predicted laser transitions in the Lyman band. This table was aided by the availability of the accurate identification of Herzberg and Howe⁷.

Excitation System

Fast rise-time, high voltage excitation sources applicable to gas lasers were not available before the developments by Shipman⁸ on the Blumlein circuit. Shipman modified Blumlein's circuit and adapted it

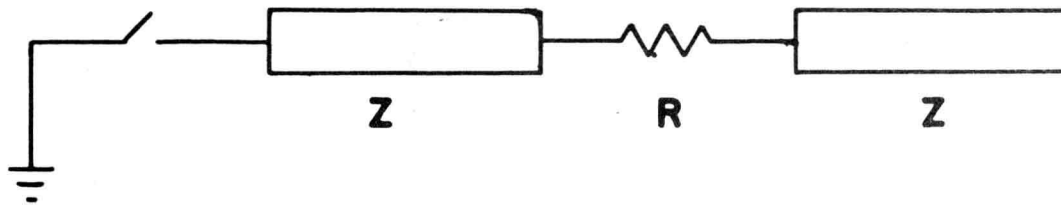


Fig. 2. Simplified version of Blumlein's circuit.

to gas lasers in an ingenious manner. Blumlein's original circuit is shown in Fig. 2, where two coaxial cables of impedance Z are separated by the load R and a switch is connected to one end of the center conductor of the cable. The cable is externally charged to voltage $+V$, and the switch is closed. The resulting short circuit causes a $-V$ voltage wave to travel toward the load and, for the case where $R \gg Z$, doubles the voltage across the load.

Starting with this circuit, Shipman constructed the device shown in Fig. 3. Flat-plate transmission lines replace the coaxial cables, the laser gas becomes the load, and solid dielectric switches are spaced equally across one edge of the flat plate. By first firing an initiating solid dielectric switch in an oil capacitor, the seven solid dielectric switches can be fired sequentially. The proper sequence is determined by precisely cutting the connecting cables at longer length intervals so that the excitation wave is inclined to the laser discharge channel between the electrodes. When the proper angle is achieved, the excitation and inversion travel down the discharge channel at precisely the speed of light. The added advantage of this technique is that none of the gas has an appreciable

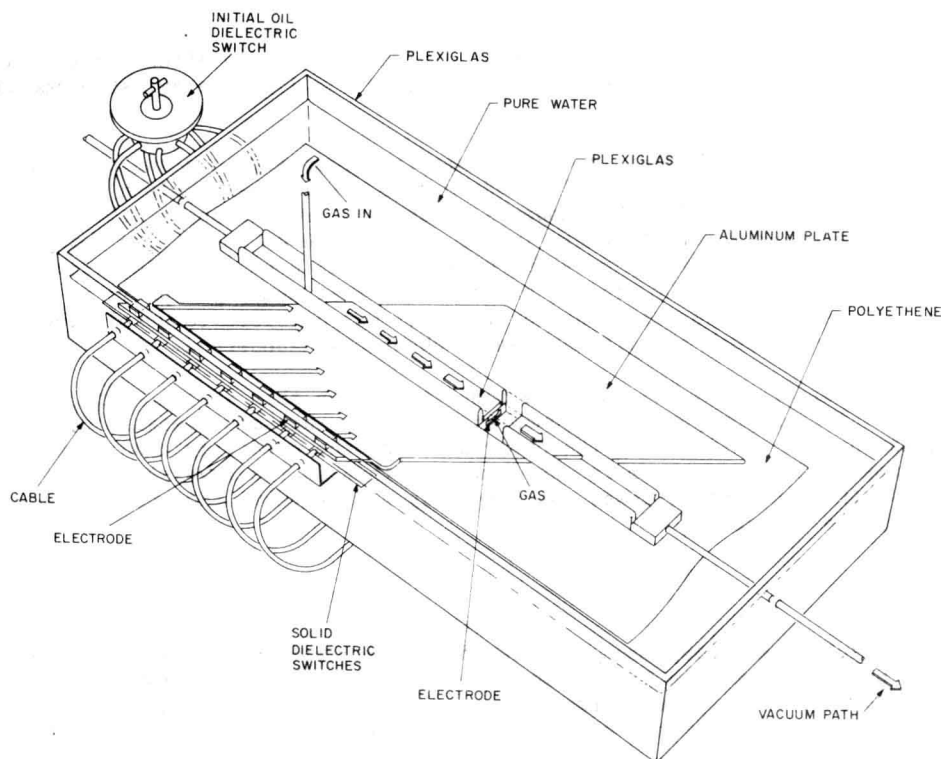


Fig. 3. Artist's sketch of the Blumlein laser.

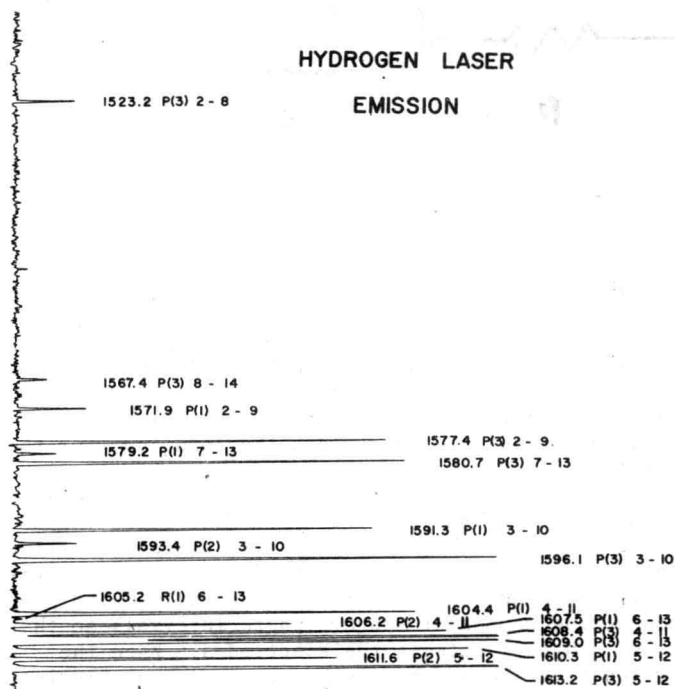


Fig. 4. Spectrogram taken of the laser emission from hydrogen.

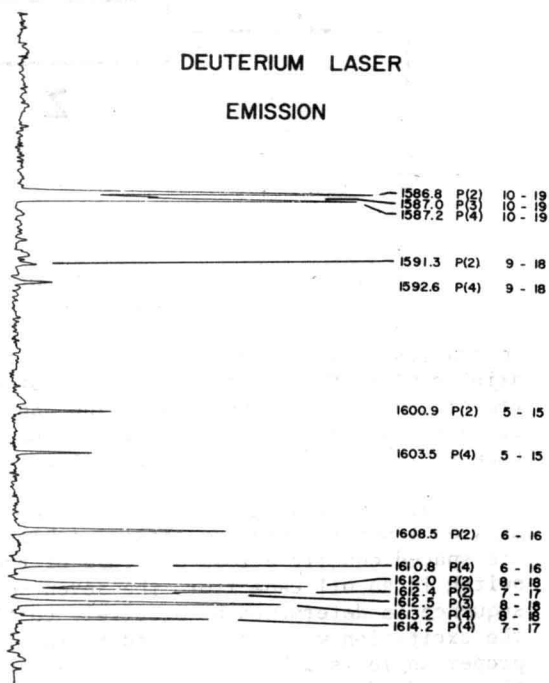


Fig. 5. Spectrogram taken of the laser emission from deuterium.

chance to decay spontaneously before the stimulated emission wave arrives to it. In effect, a traveling wave amplifier has been constructed at optical frequencies, and almost all of the emission emerges from one end of the device.

When the laser gas is H_2 , the Lyman lines shown in Fig. 4 immediately appear in a one nanosecond pulse, which contains more than a megawatt peak power. To produce this power, the Blumlein is charged to 80 kV. The resulting current of several hundred kiloamperes rises to a peak in about 2.5 nanoseconds. As pressure is varied, the maximum output occurs in the range of 20-40 torr. The detection of these fast vacuum ultraviolet pulses was aided by previous work⁹ in which decay times of vacuum ultraviolet sensitive phosphors were measured. By placing one of these fast decay phosphors in front of a fast photodiode detector and observing the resulting waveform, it was possible to unfold the approximate laser pulse width. The full width at half-maximum is about one nanosecond.

Because of its electronic similarity to H_2 , D_2 was also made to lase in this system. The observed lines are shown in Fig. 5. The output power was somewhat less, but the same pressure dependence was observed. In both gases, lasing was confirmed by the observation of the necessary condition (a), that the device emitted many times (> 20) more power in one direction than in the reverse direction, and the sufficient condition (b), that the output power was extremely sensitive to the angle between the excitation wave and the discharge channel.

Summary

The marriage of high voltage pulse technology to gas laser technology to produce traveling-wave excitation results in high peak power emission in the vacuum ultraviolet region. The traveling wave excitation system described should be of even greater importance as attempts are made to obtain shorter laser wavelengths. Several areas of science may be able to apply these laser pulses. Such

applications as in photoemission spectroscopy, photoemission microscopy, and photochemistry appear to have promise. In addition, it may be possible to use the laser as an excitation source for other lasers.

References-

1. Hodgson, R. T., *Phys. Rev. Letters*, 25, 494, 1970.
2. Waynant, R. W., Shipman, J. D. Jr., Elton, R. C. and Ali, A. W., *Appl. Phys. Letters*, 17, 383, 1970.
3. Bazhulin, P. A., Knyazev, I. N. and Petrash, G. G., *Sov. Phys. JETP*, 21, 649, 1965.
4. Ali, A. W. and Kolb, A. C., *Appl. Phys. Lett.*, 13, 259, 1968.
5. Ali, A. W., "Vacuum UV Laser from the Lyman and Werner Bands of the H₂ Molecule," The Catholic University of America, Space Science and Applied Physics Report No. 68-009, unpublished.
6. Spindler, R. J. Jr., *J. Quant. Spectrosc. Radiat. Transfer*, 9, 597, 1969.
7. Herzberg, G. and Howe, L. L., *Can. J. Phys.*, 37, 636, 1959.
8. Shipman, J. D. Jr., *Appl. Phys. Letters*, 10, 3, 1967.
9. Waynant, R. W. and Elton, R. C., "Scintillation Decay Times and Relative Sensitivities with Ultra-violet Laser Excitation," Proceedings of the International Conference on Organic Scintillators and Liquid Scintillation Counting, Ed. by C. Peng and D. Horrock, Academic Press, 1971.

Ronald W. Waynant is with the Naval Research Laboratory Select Student Program. Under this program, he has carried out research on his dissertation in the field of vacuum ultraviolet laser devices. He is just completing requirements at the Catholic University for his PhD in electrical engineering.

ROOM TEMPERATURE GaAlAs CLOSE-CONFINEMENT LASER DIODES

by

R. Gill, T. Gonda, P. Nyul, A. Limm and R. Speers
 RCA Solid State Division
 Somerville, N. J.

Introduction

Since the development of the close-confinement or single heterojunction GaAs laser structure in 1969 by Kressel and Nelson¹ and Hayashi, Panish and Foy², semiconductor injection lasers operating near room temperature have been demonstrated to be highly efficient, pulsed optical energy sources. While the first single heterojunction lasers utilized a GaAs active region, the technology was rapidly extended to (GaAl)As lasers in the composition range where the alloy system has a direct energy gap at room temperature^{3,4}.

This paper describes some of the properties of (GaAl)As single heterojunction lasers when operated between 250 and 400 K and compares the characteristics of typical (GaAl)As at room temperature with comparably constructed GaAs devices. Although recent advances in injection laser technology have demonstrated both double heterojunction^{5,6,7} and large optical cavity^{8,9} (LOC) GaAs and (GaAl)As laser structures, these devices will not be considered in this paper.

Laser Structure

A cross section of a typical (GaAl)As single heterojunction laser is shown in Fig. 1. The multilayer (GaAl)As structure is generated by the growth of two (GaAl) layers on a single crystal GaAs seed wafer by liquid phase epitaxy. The excellent match of the lattice parameters of GaAs and AlAs permits the epitaxial growth of the (GaAl)As alloy directly onto a pure GaAs substrate without the introduction of either serious strain or interface dislocations. The GaAs seed wafer is n-type, Si-doped and <100> oriented for growth. Heavily doped seed wafers having free carrier concentrations in the range of $2-3.5 \times 10^{18} \text{cm}^{-3}$ are utilized primarily to minimize the contribution of the seed wafer to the series resistance of the laser since, generally, about 50 μm of the substrate are

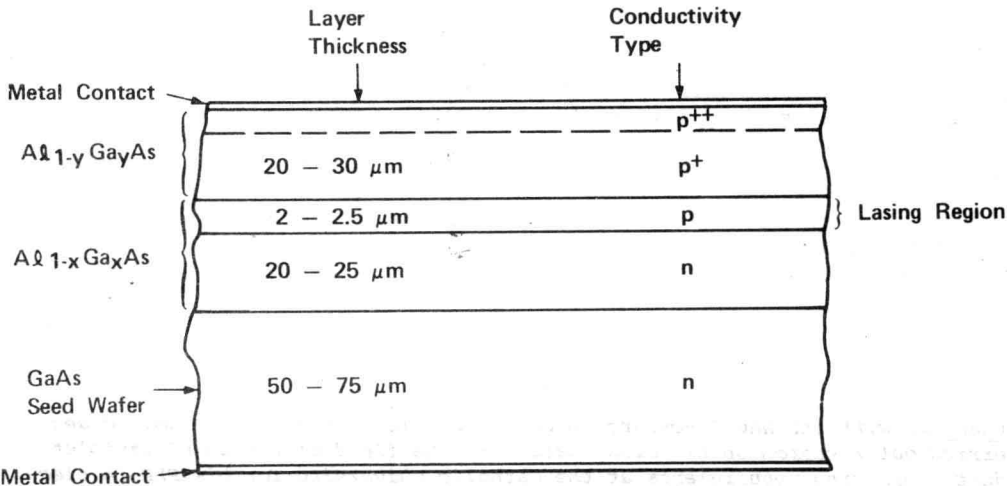


Fig. 1. Cross section of (GaAl)As single heterojunction laser.

incorporated into it. Other substrate selection criteria are similar to those utilized in the routine selection of GaAs (SH) laser substrates¹⁰.

After lapping and etching the GaAs seed wafer, an n-type (GaAl)As layer is grown on it by liquid phase epitaxy near 950 C from a melt containing Ga, As, Te and Al. This is followed by the growth of a p-type Zn-doped (GaAl)As layer on the n-layer.

To achieve the effects of the close confinement structure, the Al content and, therefore, energy band gap of this p-layer is greater than the n-layer. A post-epitaxial Zn diffusion is utilized to diffuse Zn into the n-type (GaAl)As layer and displace the p-n junction approximately 2-2.5 μm from the (GaAl)As heterojunction interface. This p-type (GaAl)As region, formed during the diffusion, defines the laser cavity and the lasing region from which the light is emitted during device operation. During the Zn diffusion process, a second Zn diffusion front, which originates at the surface of the p-type (GaAl)As epitaxial layer, forms a 5-7 μm thick p^{++} region at the surface of the p-side of the wafer. This p^{++} region provides a means of obtaining low resistance electrical contact to the p-side of the device. After a final lapping, ohmic contacts are applied to the wafers and they are cleaved into strips between 12 and 18 mils in width. To provide only single ended emission in the lasers, a reflecting optical coating is applied to one of the cleaved sides of the strips before the Fabry-Perot laser cavity is completed by wire sawing the strips into pellets of the desired size. The pellets are then soldered onto appropriate packages, which are hermetically sealed with a cap containing a transparent glass window.

General Device Results

Dependence of Lasing Threshold Current Density and Quantum Efficiency on Emission Wavelength.

In Fig. 2 is shown the wavelength and energy of emission from (GaAl)As diodes as a function of Al concentration¹¹. Although (GaAl)As has been shown to be a direct band gap semiconductor throughout the range of composition shown, the shortest wavelength at which we obtained lasing at 300 K was 7450 A.

In Fig. 3 is shown the variation of lasing threshold current density and external differential quantum efficiency with lasing wavelength at 300 K for the best units. All of these units, as well as those which will be discussed later, were single ended emitters, since they contained a reflecting optical coating on one facet of the laser cavity.

The cavity lengths of these particular units varied between 12 and 18 mils, and their emitting facets varied between 6 and 10 mils. Both the lasing threshold current density and external differential quantum efficiency of the best (GaAl)As units, which emitted between 8000 and 9000 A at 300 K, are nearly constant and compare very favorably to the best values obtained with GaAs (SH) devices¹¹.

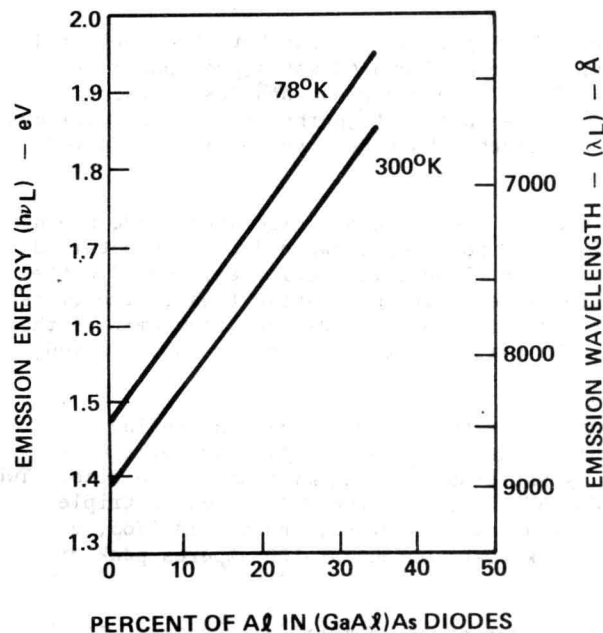


Fig. 2. Variation of wavelength and energy of emission from (GaAl)As diodes as a function of Al concentration.

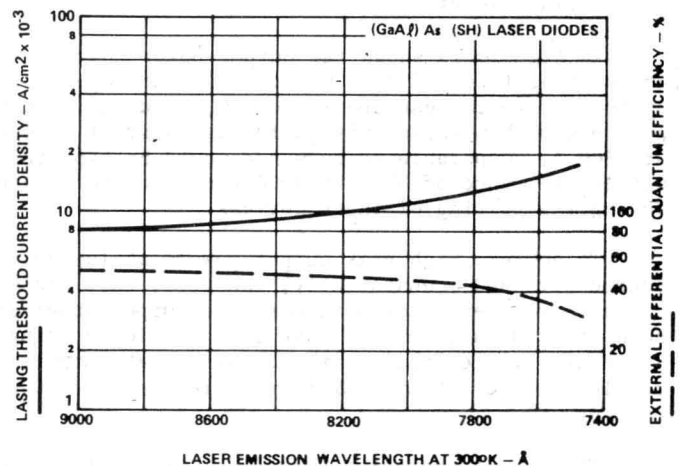


Fig. 3. Variation of lasing threshold current density and external differential quantum efficiency with wavelength for (GaAl)As lasers at 300°K.

As the (GaAl)As lasing wavelength is further reduced, the threshold current density begins to increase rapidly and the device emission decreases. In Fig. 4 is shown the performance characteristics of two near visible (GaAl)As lasers. Unit No. 1 emitted at approximately 7750 Å at room temperature and Unit No. 2 at approximately 7500 Å. Although these units exhibit normal laser properties, they tend to degrade by catastrophic damage to the laser facet at peak power emission levels substantially lower than their longer wavelength (>7800 Å) counterparts. (GaAl)As lasers emitting at wavelengths greater than 7800 Å can typically be operated at emission levels near 1 watt/mil of facet using 100 ns pulses, while devices such as those shown in Fig. 4 are frequently degraded by facet erosion at emission levels between 0.5 and 0.75 watts/mil of facet.

Temperature Dependence of (GaAl)As Laser Performance. In Fig. 5 is shown the dependence of lasing threshold current density on temperature for a (GaAl)As laser in the range 250 to 400 K. The emission wavelength of this device, which shifted about 2-3 Å per °K temperature change, was 8090 Å at 300 K. The threshold current density had an exponential dependence on temperature throughout the range investigated.

Figures 6, 7 and 8 show power output versus forward drive characteristics for three different (GaAl)As lasers at temperatures ranging from 250 to 400 K. These devices all exhibit a linear dependence of optical power output on forward drive and compare very favorably with GaAs (SH) lasers in optical efficiency and lasing threshold. The optical efficiencies and, consequently, the power efficiency of these devices decrease with increasing temperature. At 300 K, power efficiencies typically range from 4-8% for these devices. The device shown in Fig. 8, which had an output of 8 watts peak power at 45 amperes drive current at 125 C, exhibited the highest operational temperature reported to date for a (GaAl)As (SH) injection laser. At 125 C, the differential external quantum efficiency of this device dropped by about 25% from its room temperature value of 43%.

Laser Emission Pattern. A typical far field output intensity distribution of a (GaAl)As (SH) injection laser is shown in Fig. 9. This distribution pattern is characteristic of both (GaAl)As and GaAs (SH) injection lasers with lasing region thicknesses of approximately 2.5 μm. The beam divergence perpendicular to the plane of the laser junction results from diffraction of the emitted beam due to the narrow lasing region, while the smaller divergence in the plane parallel to the junction seems to be typical of all of our wire sawed lasers. For a laser emission pattern of this type, over 90% of the total power output would be collected by an f/1.0 optical system, 70% by an f/2.0 system and 50% by an f/3.0 system.

High Power Lasers and Laser Stacks. In GaAs laser technology, two designs have been utilized in fabricating room temperature optical sources that emit between 25 and 60 watts peak power -- namely, large area diodes¹², of which the RCA TA7705 and TA7787 are examples, and laser stacks formed by soldering two or three 9 or 16-mil laser pellets one on top of another to form a small compact rectangular series array of diodes. Both of these approaches have been successfully applied to (GaAl)As lasers.

In Fig. 10 is shown the output power characteristic of an experimental large area diode having an emitting facet 37 mils wide. A linear dependence of output power on forward drive was obtained up to a drive current density of 50,000 a/cm². At this current level, the device emitted 52 watts peak power when pulsed with a 100 ns pulse at a repetition rate of 100 Hz. While this device emits at 8560 Å, comparable performance would be expected for similarly designed devices that emit in the wavelength range of 8000 to 9000 Å at room temperature. No evidence of cross moding was observed during the testing of these devices.

To achieve high peak output powers at low drive currents without appreciably increasing the source size and, consequently, the size, cost and weight of the optical collection system, laser diodes have been stacked to maximize output power density while maintaining minimum source size. Two such stacked laser arrays have been developed using GaAs (SH) lasers -- the RCA TA7764, a triple stack of 9-mil emitters with 25 watts peak output power at 40 amperes drive, and the TA 7765, a double stack of 25-mil emitters, which deliver 50 watts peak power output at 100 amperes peak drive current.

The output characteristic of a triple stack (GaAl)As laser array geometrically similar to the TA 7764 is shown in Fig. 11. At room temperature, this device (which emitted at 8500 Å) had a peak

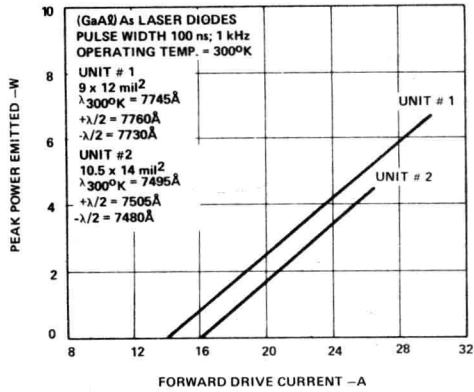


Fig. 4. Performance characteristics of near visible (GaAl)As lasers at 300 K.

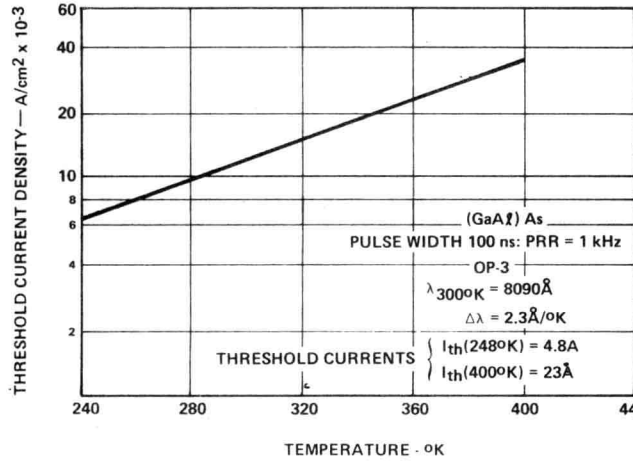


Fig. 5. Dependence of lasing threshold current density on temperature for a (GaAl)As laser from 250-400 K.

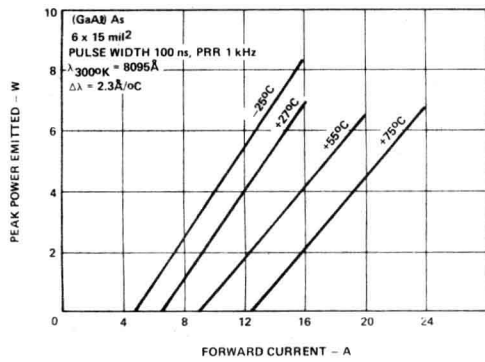


Fig. 6. Power output versus forward current for a 6-mil (GaAl)As laser from 250-350 K.

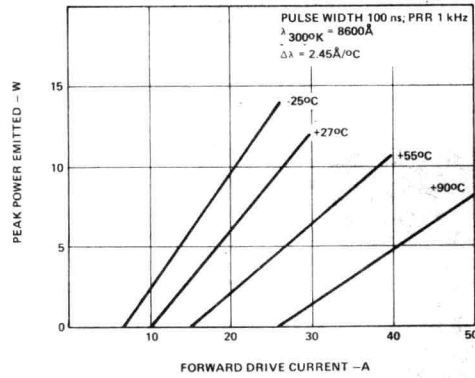


Fig. 7. Power output versus forward current for a 9-mil (GaAl)As laser from 250-365 K.

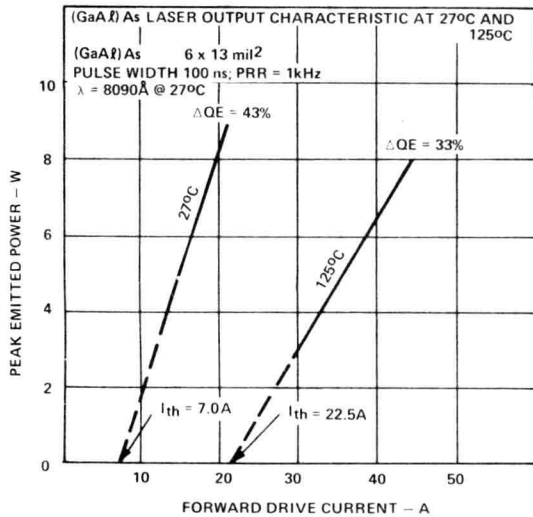


Fig. 8. Output characteristic of a (GaAl)As laser at 27 C and 125 C.

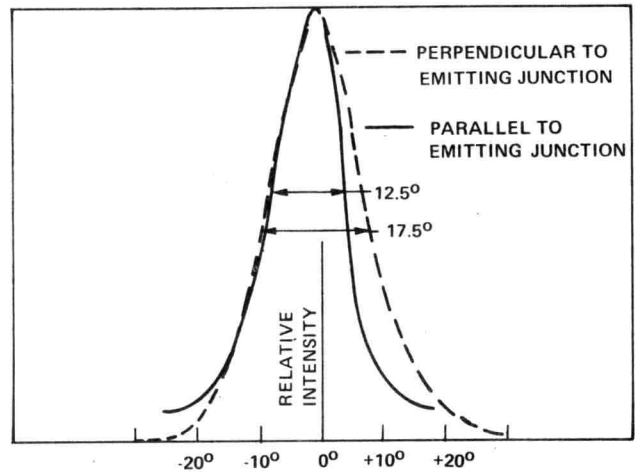


Fig. 9. Far-field emission pattern of a (GaAl)As injection laser.

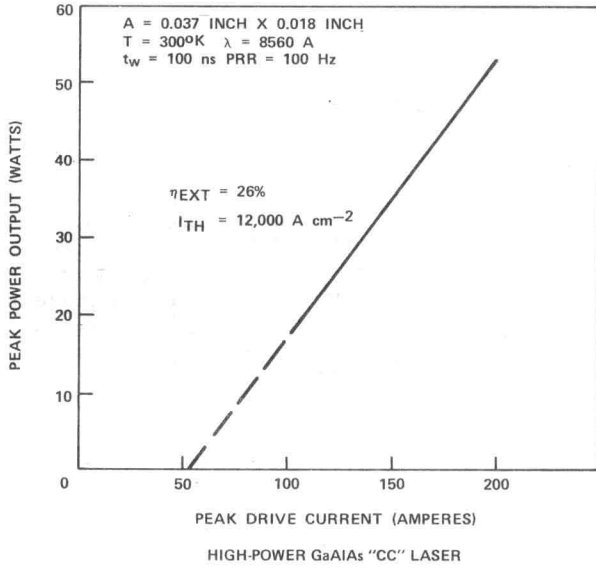
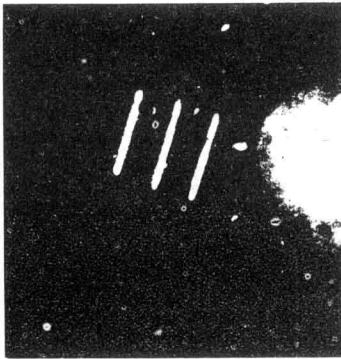


Fig. 10. Power output versus forward drive of a high power (GaAl)As "CC" laser.



IR EMISSION (EMITTING
 AREA: 9 BY 9 MILS)
 THREE-PELLET (9- BY
 12-MIL) STACKED LASER
 DIODE

Fig. 12. Near-field emission pattern of a GaAs triple laser stack.

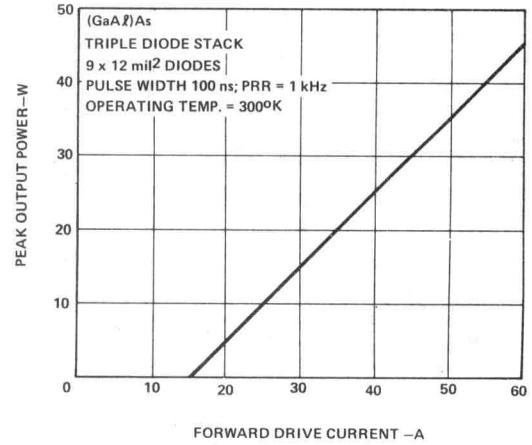


Fig. 11. Optical power output versus forward drive of a (GaAl)As triple diode stack.

output power of 26 watts when driven at 40 amperes with a 100 ns current pulse at 1 kHz repetition rate. The near field emission pattern for a triple pellet array of the same geometry, consisting of GaAs lasers, is shown in Fig. 12. As seen in this photograph, the array forms a compact optical source approximately 9 mils square.

Standard (GaAl)As Lasers and Laser Arrays

Discrete Devices. Two (GaAl)As discrete lasers have been standardized and are available for operation at and near room temperature -- the TA7867, a 6-mil laser, and the TA8127, a 9-mil laser. These devices are compared in Table 1 with standard GaAs (SH)

Table 1. Comparison of characteristics of (GaAl)As lasers with GaAs lasers.

RCA DEV. NO'S.	TA7607	TA7608	TA7867	TA7609	TA7610	TA8127
MATERIAL	GaAs	GaAs	GaAlAs	GaAs	GaAs	GaAlAs
Emission Wave Length	9050Å	9050Å	8000Å-9000Å	9050Å	9050Å	8000Å-9000Å
Pellet Size (mil ²)	6 x 12	6 x 12	6 x 12	9 x 12	9 x 12	9 x 12
Threshold Current	6	6	10	10	10	15
Peak Forward Current (A)	20	25	25	30	40	40
Total Radiant Peak Power Output (W)	6	6	5	13	13	10
Pulse Duration (ns)	200	200	100	200	200	100